Nuclear Instruments and Methods in Physics Research B 279 (2012) 84–91

Contents lists available at SciVerse ScienceDirect

Nuclear Instruments and Methods in Physics Research B

journal homepage: www.elsevier.com/locate/nimb

Spatially resolved transport data for electrons in gases: Definition, interpretation and calculation

S. Dujko [a,b,c,*], R.D. White [b], Z.M. Raspopović [a], Z.Lj. Petrović [a]

[a] Institute of Physics, University of Belgrade, P.O. Box 68, Pregrevica 118, 11080 Belgrade, Serbia
[b] ARC Centre for Antimatter-Matter Studies, School of Engineering and Physical Sciences, James Cook University, Townsville 4810, Australia
[c] Centrum Wiskunde & Informatica (CWI), P.O. Box 94079, 1090 GB, Amsterdam, The Netherlands

ARTICLE INFO

Article history:
Received 22 July 2011
Received in revised form 4 October 2011
Available online 25 November 2011

Keywords:
Electron swarms
Transport properties
Boltzmann equation
Monte Carlo simulation

ABSTRACT

The spatiotemporal evolution of electron swarms in the presence of electric and magnetic fields is investigated to facilitate understanding temporal and spatial non-locality in low-temperature plasmas. Using two independent techniques, a multi-term solution of Boltzmann's equation and a Monte Carlo simulation technique, the synergism of an applied magnetic field and non-conservative collisions (ionization and/or electron attachment) is demonstrated as a means to control the non-locality of relaxation processes. In particular, oscillatory features in the spatial and temporal profiles are demonstrated, and shown to be enhanced or suppressed through the magnetic field strength, the angle between the electric and magnetic fields, and the degree of ionization. Finally we discuss the impact of field configurations and strengths on the transport properties, highlighting the distinctions in the measured transport properties between various experimental configurations when non-conservative processes are present.

1. Introduction

The theoretical investigation of charged-particle transport processes in neutral gases under the influence of electric and magnetic fields is a topic of great interest both as a problem in basic physics and for its potential for application to modern technology [1,2]. One of the major challenges in these investigations is an accurate representation of the spatiotemporal evolution of the phase-space distribution function and the associated transport properties of an electron swarm moving under the influence of electric and magnetic fields. Relaxation processes in electron swarms are related to various problems of gaseous electronics such as modeling of non-equilibrium plasma discharges [3–6], modeling of gaseous detectors of elementary particles [7], modeling of transient phenomena in swarm physics [8–12] and physics of gas lasers [13]. In the plasma modeling community, it is well known that within many plasma discharges sustained and controlled by electric and magnetic fields, these fields can vary in space, time and orientation depending on the type of discharge. Although there has been a tremendous amount of research into temporal and spatial non-locality of electron transport for conservative systems and electric field only situations (see, e.g., [6,12,14,15] and references therein), the study of the spatiotemporal development of an electron swarm where magnetic fields are included explicitly and when the transport is greatly affected by non-conservative collisions (collisions where the number of particles that are modeled changes, e.g., ionization and/or electron attachment) has not been developed to such a level. First, this may be due to the unavoidable additional complexity associated with introducing a magnetic field into the theories and simulations (see e.g., [12,16–19]). Second, investigations related to the effects of non-conservative collisions on the spatiotemporal development of the electron swarm are very few. Under steady-state Townsend conditions (SST), where large spatial gradients in number density of charged particles exist in the vicinity of electrodes or in the vicinity of disturbing sources, Li et al. [20], Dujko et al. [21] and Takeda and Ikuta [22] have considered the explicit effects of ionization and attachment on the spatial relaxation profiles for the ionization model of Lucas and Saelee [23]. It was shown that both the ionization and attachment processes strongly affect the relaxation profiles and further relations required for the conversion of hydrodynamic transport properties to those found in the SST experiment were also identified [21]. However, in some cases, a knowledge of both the spatial and temporal development of electron swarm properties is required, for example to investigate the transient phenomena and relaxation times/lengths in a bounded plasma discharge or to analyze the electron kinetics in space and/or time varying electric and magnetic fields. The spatiotemporal development of electron swarms also has implications for the correct implementation of transport data in fluid models of plasma discharges, particularly under

* Corresponding author at: Institute of Physics, University of Belgrade, P.O. Box 68, Pregrevica 118, 11080 Belgrade, Serbia. Tel.: +381 11 3713001; fax: +381 11 3162190.
E-mail address: sasa.dujko@ipb.ac.rs (S. Dujko).

0168-583X/$ - see front matter © 2011 Elsevier B.V. All rights reserved.
doi:10.1016/j.nimb.2011.10.067

conditions where the local field approximation is of limited applicability due to large spatial and/or temporal variation in the electric and magnetic fields. On a more fundamental level, the spatiotemporal evolution of electron swarms has implications for how the measured swarm transport properties under different experimental conditions should be calculated and interpreted [21,24].

We begin this paper with a brief review of multi-term theory for solving the non-conservative Boltzmann equation involving spatiotemporal variations when electric and magnetic fields are present and crossed at arbitrary angles. In addition to the Boltzmann equation analysis, we discuss our Monte Carlo method for electrons under both hydrodynamic and non-hydrodynamic conditions and incorporating the effects of non-conservative collisional processes. We focus on two situations: (i) spatiotemporal development of a pulse of electrons, and (ii) spatial relaxation of electrons under the SST conditions. After giving brief reviews of theoretical methods, we then provide numerical examples for certain model and real gases of special interest, highlighting recent new results.

2. Theory

2.1. Boltzmann equation analysis

The behavior of electrons in gases under the influence of electric and magnetic fields is described by the phase-space distribution function $f(\boldsymbol{r},\boldsymbol{v},t)$ representing the solution of the Boltzmann equation

$$\frac{\partial f}{\partial t}+\boldsymbol{c}\cdot\frac{\partial f}{\partial \boldsymbol{r}}+\frac{q}{m}[\boldsymbol{E}+\boldsymbol{c}\times\boldsymbol{B}]\cdot\frac{\partial f}{\partial \boldsymbol{c}}=-J(f,f_0), \tag{1}$$

where $\boldsymbol{r}$ and $\boldsymbol{c}$ denote the position and velocity co-ordinates, q and m are the charge and mass of the swarm particle and t is time. The electric and magnetic fields are assumed spatially homogeneous with magnitudes E and B, respectively. In what follows, we employ a co-ordinate system in which $\boldsymbol{E}$ defines the z-direction while $\boldsymbol{B}$ lies in the y–z plane, making an angle ψ with respect to $\boldsymbol{E}$. Swarm conditions are assumed to apply and $J(f,f_0)$ denotes the rate of change of f due to binary collisions with the neutral molecules only. The original Boltzmann collision operator [25] and its semiclassical generalization [26] are used for elastic and inelastic processes, respectively. The attachment and ionization collision operators employed are detailed in [27,28].

The directional dependence of f in velocity space is represented by an expansion in terms of spherical harmonics:

$$f(\boldsymbol{r},\boldsymbol{c},t)=\sum_{l=0}^{\infty}\sum_{m=-l}^{l}f_m^{[l]}(\boldsymbol{r},c,t)Y_m^{[l]}(\hat{\boldsymbol{c}}), \tag{2}$$

where $Y_m^{[l]}(\hat{\boldsymbol{c}})$ are spherical harmonics and $\hat{\boldsymbol{c}}$ denotes the angles of $\boldsymbol{c}$. The errors associated with the two-term approximation (when the distribution function significantly deviates from isotropy in velocity space) and inadequacies of a Legendre polynomial expansion (when density gradients are not parallel to the field) are highlighted in our previous publications [1,12,18,28] and avoided in this work.

The speed dependence of the coefficients $f_m^{[l]}(\boldsymbol{r},c,t)$ can be represented in a variety of ways [28]. In this work, we use an expansion around a Maxwellian at an arbitrary basis temperature T_b in terms of modified Sonine polynomials [12,18]. For time-dependent fields, the basis temperature is also time dependent, e.g., $T_b=T_b(t)$ and used to optimize convergence of this expansion. Under the hydrodynamic conditions [29–31], the spatial dependence of f is treated by the familiar density gradient expansion:

$$f(\boldsymbol{r},\boldsymbol{c},t)=\sum_{s=0}^{\infty}f^{(s)}(\boldsymbol{c},t)\odot(-\nabla)^s n(\boldsymbol{r},t). \tag{3}$$

The continuity of charged particles in phase-space requires

$$\frac{\partial n}{\partial t}+\nabla\cdot\boldsymbol{\Gamma}(\boldsymbol{r},t)=S(\boldsymbol{r},t), \tag{4}$$

where $\boldsymbol{\Gamma}$ is the charged particle flux and $S(\boldsymbol{r},t)$ is the production rate per unit volume per unit time arising from non-conservative processes. Assuming the functional relationship (3) the flux and source term could be also expanded in terms of powers of the density gradients:

$$\boldsymbol{\Gamma}(\boldsymbol{r},t)=\boldsymbol{W}^{\star}(t)n(\boldsymbol{r},t)-\boldsymbol{D}^{\star}(t)\cdot\nabla n(\boldsymbol{r},t)+\cdots, \tag{5}$$

$$S(\boldsymbol{r},t)=S^{(0)}(t)n(\boldsymbol{r},t)-\boldsymbol{S}^{(1)}(t)\cdot\nabla n(\boldsymbol{r},t)+\boldsymbol{S}^{(2)}(t):\nabla\nabla n(\boldsymbol{r},t)+\cdots, \tag{6}$$

where $\boldsymbol{W}(t)^{\star}$ and $\boldsymbol{D}^{\star}(t)$ define, respectively, the *flux* drift velocity and *flux* diffusion tensor. Substitutions of expansions (5) and (6) into the continuity Eq. (4) results in truncation the second order in the density gradients, the time-dependent diffusion equation:

$$\frac{\partial n}{\partial t}+\boldsymbol{W}(t)\cdot\nabla n-\boldsymbol{D}(t):\nabla\nabla n=-R_a(t)n, \tag{7}$$

where $R_a(t)$, $\boldsymbol{W}$(t) and $\boldsymbol{D}$(t) are, respectively, the loss rate coefficient, *bulk* drift velocity, and the *bulk* diffusion tensor. These transport properties contain explicit contributions from non-conservative collisions and are given by

$$R_a(t)=S^{(0)}(t)-\int J^R[f^{(0)}(\boldsymbol{c},t)]d\boldsymbol{c}, \tag{8}$$

$$\boldsymbol{W}(t)=\boldsymbol{W}^{\star}(t)-\boldsymbol{S}^{(1)}(t)=\int\boldsymbol{c}[f^{(0)}(\boldsymbol{c},t)]d\boldsymbol{c}-\int J^R[f^{(1)}(\boldsymbol{c},t)]d\boldsymbol{c}, \tag{9}$$

$$\boldsymbol{D}(t)=\boldsymbol{D}^{\star}(t)-\boldsymbol{S}^{(2)}(t)=\int\boldsymbol{c}[f^{(1)}(\boldsymbol{c},t)]d\boldsymbol{c}-\int J^R[f^{(2)}(\boldsymbol{c},t)]d\boldsymbol{c}, \tag{10}$$

where J^R denotes the reactive part of the collision operator.

The bulk transport coefficients are measured and tabulated in swarm experiments. From Eqs. (9) and (10), it is clear that the bulk drift velocity is associated with the rate of change of the position of the center-of-mass of the swarm while the bulk diffusion coefficient describes the rate of change of spread of the swarm about its center-of-mass. The explicit influence of non-conservative collisions on the swarm's center-of-mass transport is described by the terms $\boldsymbol{S}^{(1)}$ and $\boldsymbol{S}^{(2)}$. Obviously, in the absence of non-conservative collisions, the bulk and flux transport coefficients coincide. One should be aware of the differences in the definitions of both sets of transport coefficients, and ensure that the data employed in their models is consistent with data required by their models. The results in Section 3 demonstrate the large differences frequently observed between these two sets of data. In plasma modeling, the most appropriate procedure would be to use the experimental swarm data (e.g., bulk transport coefficients) for the analysis of the validity of the cross sections and then to calculate the flux transport coefficients which are necessary as input data in fluid modeling of plasma discharges.

To determine all the transport coefficients defined in Eqs. (8)–(10) in the presence of non-conservative collisions, truncation of Eq. (3) at $s=2$ is necessary. This, together with Eq. (1) yields a hierarchy of coupled kinetic equations. Comprehensive details of the hydrodynamic theory and numerical procedure when both the electric and magnetic fields are present, are given in our previous publications [1,12,18].

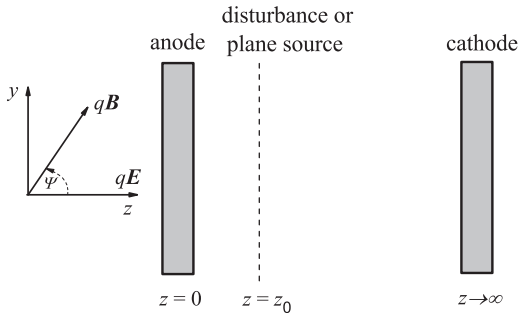

Fig. 1. Schematic representation of an idealized steady-state Townsend experiment considered in this work.

In many plasma discharges, however, the existence of sources and/or sinks, physical boundaries and/or spatially varying fields can give rise to *non-hydrodynamic* behavior. In this case, the spatial dependence of the distribution function must be treated explicitly and the density gradient expansion given by Eq. (3) is of limited applicability. In this work, we consider an idealized SST experiment, schematically represented in Fig. 1. The charged particles are emitted at a constant rate from an infinite plane source at $z = z_0$ and interact with the neutral gas under the influence of spatially uniform electric and magnetic fields, generally crossed at arbitrary angles. The steady-state Boltzmann equation must be solved and here we use a second-order, finite differencing scheme with appropriate modifications at the boundaries to solve the generated hierarchy of kinetic equations. The boundary conditions on the distribution function are detailed in [14,19]. The explicit expressions for the space-dependent transport properties are given in our previous publications [12,14].

2.2. Monte Carlo method

In this work we apply a Monte Carlo simulation code that follows a large number of electrons (typically 10^5–10^6) through a neutral gas under the influence of spatially homogeneous electric and magnetic fields. Electrons gain the energy from the external electric field and dissipate it through collisional transfer to the neutral gas molecules by elastic and different types of inelastic collisions, including reactive collisions. Under the hydrodynamic conditions, it is assumed that an electron swarm develops in an infinite space. Under the SST conditions, the primary electrons are released one by one from the disturbing source into the half space. In the present Monte Carlo code we follow the spatiotemporal evolution of each electron through time steps governed by the minimum of two relevant time constants: mean collision time and cyclotron period for the $\boldsymbol{E} \times \boldsymbol{B}$ field. These finite time steps are used to solve the integral equation for the collision probability in order to determine the time of the next collision. Once the moment of the next collision is established, the nature of the collision is determined by using the relative probabilities of the various collision types. All electron scattering are assumed to be an isotropic regardless of the collision nature, specific process and energy.

In order to follow the spatiotemporal development of the electron swarm under the influence of spatially homogeneous electric and magnetic fields under hydrodynamic conditions, we have restricted the space and divided it into boxes. Every box contains 100 points and these points are used to sample spatial parameters of the electron swarm. This concept of our code enabled us to follow the development of the swarm in both real space and normalized to 6σ, where σ is the standard deviation of the Gaussian distribution in space. The spatially resolved electron transport properties including the average energy/velocity have been determined by counting the charged particles and their energies/velocities in every cell. Therefore, we may follow the spatial profiles of electron positions as well as spatial profiles of the average energy/velocity as they develop in space and time and within the swarm.

Under the non-hydrodynamic conditions when both the explicit and implicit gradients in charged particle number density exist, the sampling of spatially resolved transport data for electrons is not so simple. In particular, under the SST conditions along different points of a discharge there exist different electrons originating from the source at different times. In order to describe this physical situation accurately, the principal axis z has been divided into a large number of small boxes of width Δz and infinite over perpendicular axes. Any property may be defined in jth box (i.e., between $z_j - \Delta z/2$ and $z_j + \Delta z/2$) as:

$$\langle \xi \rangle_j = \left(\frac{1}{\Delta z} \int_{z_j - \Delta z/2}^{z_j + \Delta z/2} f_{SST}(z, \boldsymbol{v}) d\boldsymbol{r} d\boldsymbol{v} \right)^{-1} \times \frac{1}{\Delta z} \int_{z_j - \Delta z/2}^{z_j + \Delta z/2} \xi f_{SST}(z, \boldsymbol{v}) d\boldsymbol{r} d\boldsymbol{v}$$
$$\approx \left(\sum_{k=1}^{N} \Delta t_k^j \right)^{-1} \sum_{k=1}^{N} \xi_k^j \Delta t_k^j, \tag{11}$$

where $f_{SST}(z, \boldsymbol{v})$ is the steady state distribution function, ξ_k^j is the value of the quantity to be sampled when the kth electron is contained in the jth box, Δt_k^j is the residence time of the electron in that box, and N is the total number of electrons that appear there. The reasons why the residence time of the electrons must be considered in the above sampling formula are given in [33]. For further details the reader is referred to Dujko et al. [21].

3. Results and discussion

3.1. The transition to the hydrodynamic regime: spatiotemporal evolution of a pulse of charged swarm particles

In this section we study how hydrodynamic conditions develop in space and time for a pulse of electrons in an unbounded gas, similar in nature to the traditional time-of-flight experiment. In addition, we present two examples of hydrodynamic transport coefficients obtained in the hydrodynamic limit, which show the simultaneous effects of magnetic fields and non-conservative collisions. It should be emphasized that to study the transition to hydrodynamic conditions, we cannot use the simplifying methods developed to study hydrodynamic conditions (viz. density gradient expansions), and the full space–time variation of the distribution function must be sampled/calculated.

To understand the fundamental effects of ionization on the spatiotemporal development of the electron transport properties we consider electrons in the ionization model of Lucas–Saelee model [23]. In this model, the cross sections are specified as follows:

$$\sigma_e(\epsilon) = 4\epsilon^{-1/2}\ \text{Å}^2$$
$$\sigma_{ex}(\epsilon) = \begin{cases} 0.1(1-F)(\epsilon - 15.6)\ \text{Å}^2, & \geqslant 15.6\ \text{eV} \\ 0, & \epsilon < 15.6\ \text{eV} \end{cases} \tag{12}$$
$$\sigma_I(\epsilon) = \begin{cases} 0.1F(\epsilon - 15.6)\ \text{Å}^2, & \geqslant 15.6\ \text{eV} \\ 0, & \epsilon < 15.6\ \text{eV} \end{cases},$$

where σ_e, σ_{ex} and σ_I are the cross sections for elastic, inelastic and ionization collisions, respectively. Other details of the model include $\epsilon_i = 15.6$ eV, $T_0 = 0$ K, $m/M = 10^{-3}$ where m and M denote the electron and molecular mass, respectively. The parameter F controls the magnitude of the cross sections for inelastic collisions and ionization: if $F = 0$, no ionization occurs, if $F = 0.5$ the cross sections for excitation and ionization are equal and finally if $F = 1$, no excitation occurs.

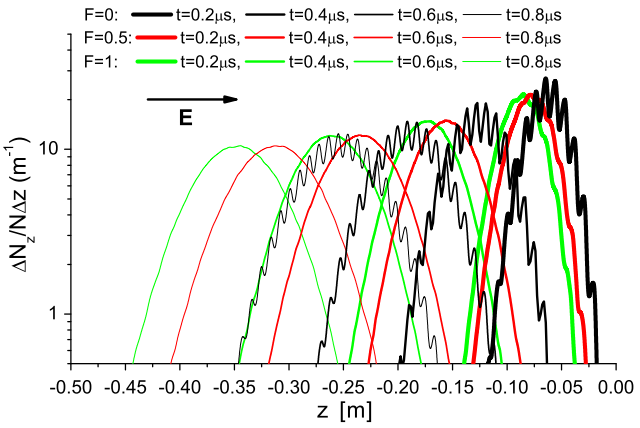

Fig. 2. Spatiotemporal profiles of the density profiles for the instants 0.2, 0.4, 0.6 and 0.8 μs for the ionization model of Lucas and Saelee as a function of parameter *F*.

Fig. 2 displays the spatiotemporal development of a swarm of charged particles along the electric field direction for the ionization model of Lucas and Saelee. The reduced electric field E/n_0 (where n_0 is the gas number density and is set to 3.54×10^{22} m^{-3} which corresponds to the pressure of 1 Torr at 273 K) is 50 Td (1 Td = 10^{-21} Vm^2). The spatial density profiles are normalized using a total number of charged particles for a given instant of time. Fig. 3(a and b) illustrates spatiotemporal development of the average energy along the swarm. We see that parameter *F* strongly affects the spatiotemporal development of the swarm. For $F = 0$, the existence of oscillatory features in the profiles of the spatial distribution of particles and average energy is clearly evident. The transient spatial structures in the density and average energy are similar to those observed in the steady-state Townsend and Franck–Hertz experiments [20,21,34]. The basic characteristics of these oscillations are controlled by strong competition between elastic and inelastic energy losses. If the collisional energy loss is governed essentially by 'continuous' energy loss processes then there are no oscillations in the profiles (e.g., when the mean swarm energy is much less than the lowest energy threshold and elastic collisional processes are dominant, or when mean swarm energies are much greater than the lowest energy threshold) while if the collisional energy loss is dominated by 'discrete' energy loss processes then we have an oscillatory behavior in the profiles.

When the ionization degree *F* is increased, the oscillatory feature in the profiles is significantly reduced even though the total cross section for non-elastic processes remains unchanged. In addition, we observe that the average energy decreases when increasing *F*, particularly at the leading edge of the swarm. This decrease of the local mean energy and transition from oscillatory to non-oscillatory spatiotemporal profiles is caused by the energy dilution effect associated with the ionization processes [35]. After an ionization process, the remaining energy is always shared between two electrons, while in the case of an inelastic collision, the remaining energy is held only by one electron. As a consequence, the mean energy after ionization is lower than that after an inelastic collision, a phenomenon usually called energy dilution due to ionization. The remaining two slow electrons undergo more elastic collisions which always tend to damp this oscillatory behavior. In the literature, it is not unusual for ionization to be treated as merely another conservative inelastic collisional process, entirely ignoring the effect of particle production. If this approximation were to hold in our calculations, there would have been no variation in the calculated profiles with respect to *F*.

Another interesting point is to compare the relaxation times for different processes. Transport coefficients (mean energy, drift velocity and diffusion coefficients) are fully relaxed after 25 ns for the case where $F = 0.5$ and E/n_0 of 50 Td. Our careful analysis based on a Boltzmann equation analysis and Monte Carlo simulations has revealed that an oscillatory feature in the profiles is still present. The oscillatory feature in the profiles of the energy distribution function and associated swarm parameters is removed after approximately 500 ns. However, even under these conditions, the swarm is not fully relaxed in space due to the presence of significant diffusive fluxes induced by the gradients in the number density of charged particles. It is found that the full spatial relaxation is achieved under conditions when diffusion fluxes due to gradients in electron number density are much less than the corresponding drift due to the electric field force. Only under these conditions, the swarm is fully relaxed in space and local velocities at the leading and trailing edges of the swarm remain unchanged in time.

In Fig. 4 we illustrate the impact of an orthogonal magnetic field on the spatial density profile and spatially-resolved energy distribution function for the ionization model of Lucas and Saelee. The parameter *F* is set to 0.5 while $E/n_0 = 50$ Td and the profiles are shown for the instant of 0.1 μs. When the reduced magnetic field of 250 Hx (1 Hx = 10^{-27} Tm^3) is applied the swarm is more localized in space due to the explicit orbital effect which acts to inhibit diffusion in a plane perpendicular to the magnetic field. As a consequence, the number of periodic structures is less than for magnetic field-free case; however, the oscillatory feature is more

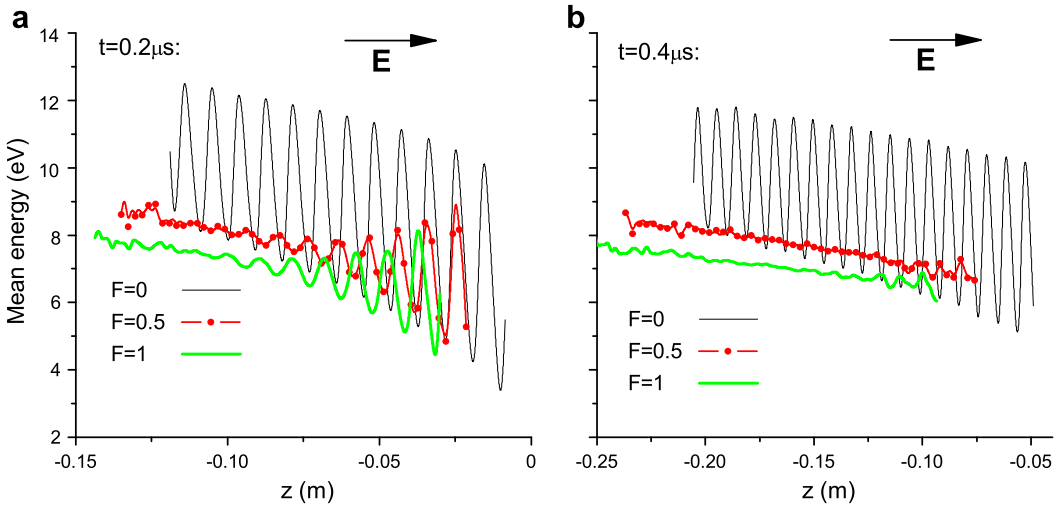

Fig. 3. Spatiotemporal profiles of the mean energy for the instants of 0.2 and 0.4 μs for the ionization model of Lucas and Saelee as a function of parameter *F*.

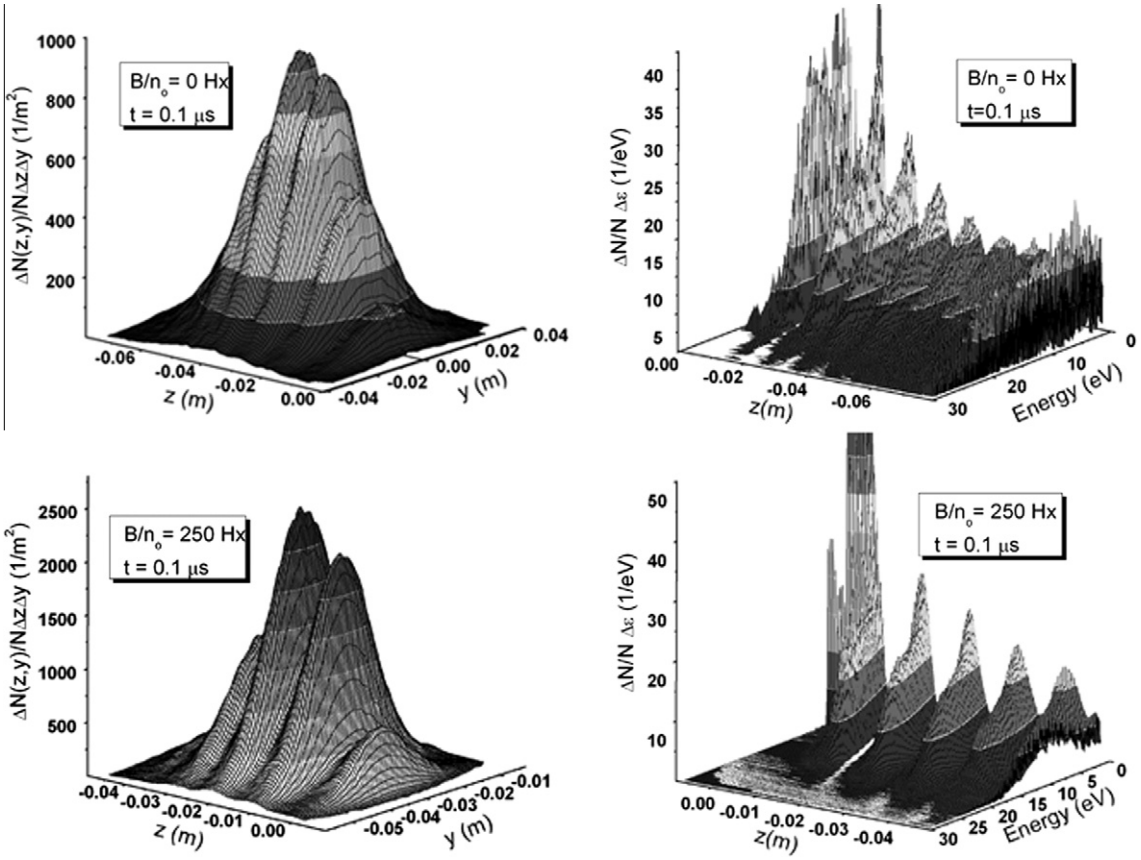

Fig. 4. Spatial density profiles and spatially-resolved distribution functions for magnetic field-free case and B/n_0 of 250 Hx for the instant 0.1. Calculations are performed for the ionization model of Lucas and Saelee ($F = 0.5$) and E/n_0 of 50 Td.

pronounced. We see that a swarm of charged particles for magnetic field-free case is symmetric with respect to x-axis. When magnetic field is applied, the swarm is shifted towards the $-x$ direction determined by the $\boldsymbol{E} \times \boldsymbol{B}$ drift. From the profiles of the energy distribution function, it is seen that the most energetic electrons are localized at the leading edge of the swarm. The application of a magnetic field leads to severe spatial segregation of the electrons and depopulation of the high energy electrons from the tail of the energy distribution function.

In order to illustrate the importance of investigating the spatio-temporal development of a swarm of charged particles and associated spatially-resolved data, in Fig. 5 we display the steady-state transport parameters as a function of E/n_0 and B/n_0 for the ionization model of Lucas and Saelee in a crossed field configuration. The parameter F is set to 0.5 and all calculations are performed for zero gas temperature. The mean energy is a decreasing function of B/n_0 due to the well-known phenomenon of magnetic cooling. This phenomenon results from an inability of the electric field to efficiently pump the energy into the swarm as B/n_0 increases. Only in the limit of high values of E/n_0 where the collision frequency is much higher than the cyclotron frequency, the mean energy shows little sensitivity with respect to the magnetic field. A similar behavior is exhibited in the ionization rate. The explicit effects of ionization are clearly evident from the profiles of the longitudinal drift velocity and longitudinal diffusion coefficient. We see that ionization starts to affect W_E and $n_0 D_{zz}$ for E/n_0 greater than 5 Td. The value of E/n_0 for which this occurs increases with B/n_0. The bulk components dominate the flux components and differences between these two sets of data can be up to 30%. The distinction between flux and bulk components of both drift velocity vector elements and diagonal elements of the diffusion tensor is a consequence of spatially dependent ionization processes resulting from a spatial variation of average electron energies within the swarm (see Fig. 3). For the present model, the ionization rate is an increasing function of electron energy, and hence electrons are preferentially created in regions of higher energy. This results in a shift in the center of mass position as well as a modification of the spread about the center of mass.

3.2. Non-hydrodynamic regime: spatial relaxation of electrons under SST conditions

In this section we extend previous work on the idealized SST experiment to include the explicit influence of a magnetic field when the electric and magnetic fields are crossed at arbitrary angles. As an illustrative example of spatial relaxation processes for electrons in real gases, we consider spatial relaxation in the mixtures of argon and molecular gases.

To understand the synergism of elastic and inelastic collisions on the one hand, and the angle between the electric and magnetic fields on the other hand, on the spatial relaxation of electrons we use the so-called step model, previously employed by Li et al. [19]. The details of this model are

$$\begin{aligned} &\sigma_m = 6\ \text{Å}^2, \\ &\sigma_i = 0.1\ \text{Å}^2\ \ \epsilon_i = 2\ \text{eV}, \\ &m_0 = 4\ \text{amu}\ \ T_0 = 0\text{K}, \end{aligned} \tag{13}$$

where the inelastic collisions are characterized by a cross section σ_i and a threshold ϵ_i while σ_m is the cross section for elastic collisions.

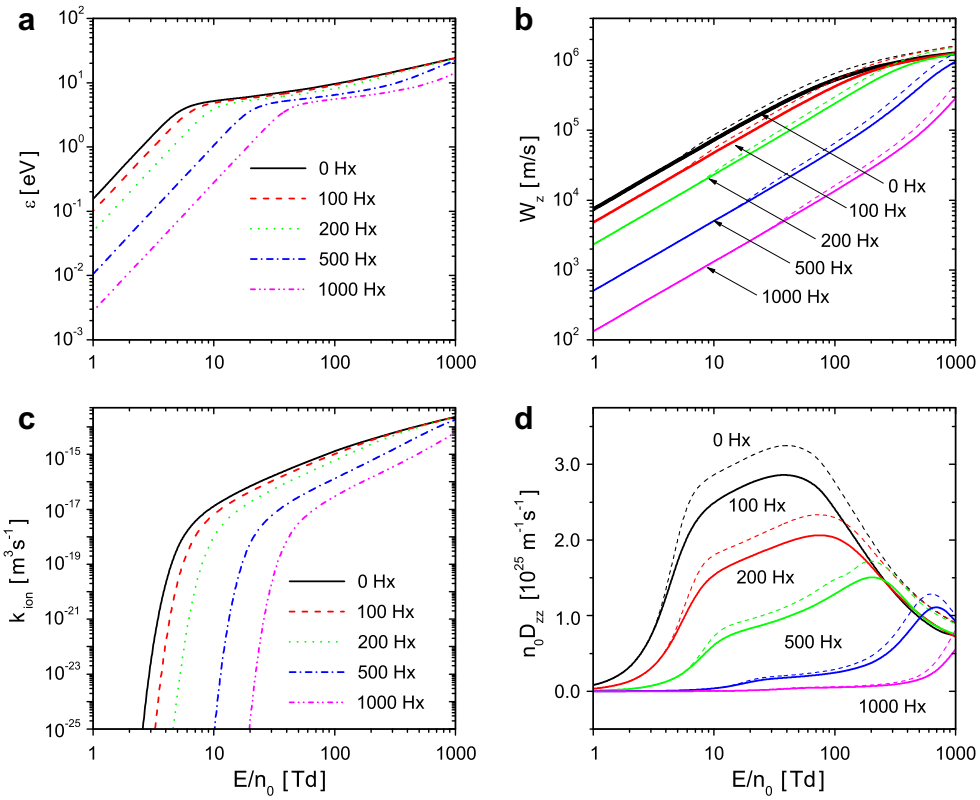

Fig. 5. Variation of the mean energy (a), longitudinal drift velocity component (b), ionization rate (c) and longitudinal diffusion coefficient (d) with E/n_0 and B/n_0 in a crossed field configuration for the ionization model of Lucas and Saelee ($F = 0.5$). Bulk values in (b) and (d) are represented with the full lines while for the flux values, dashed lines are used.

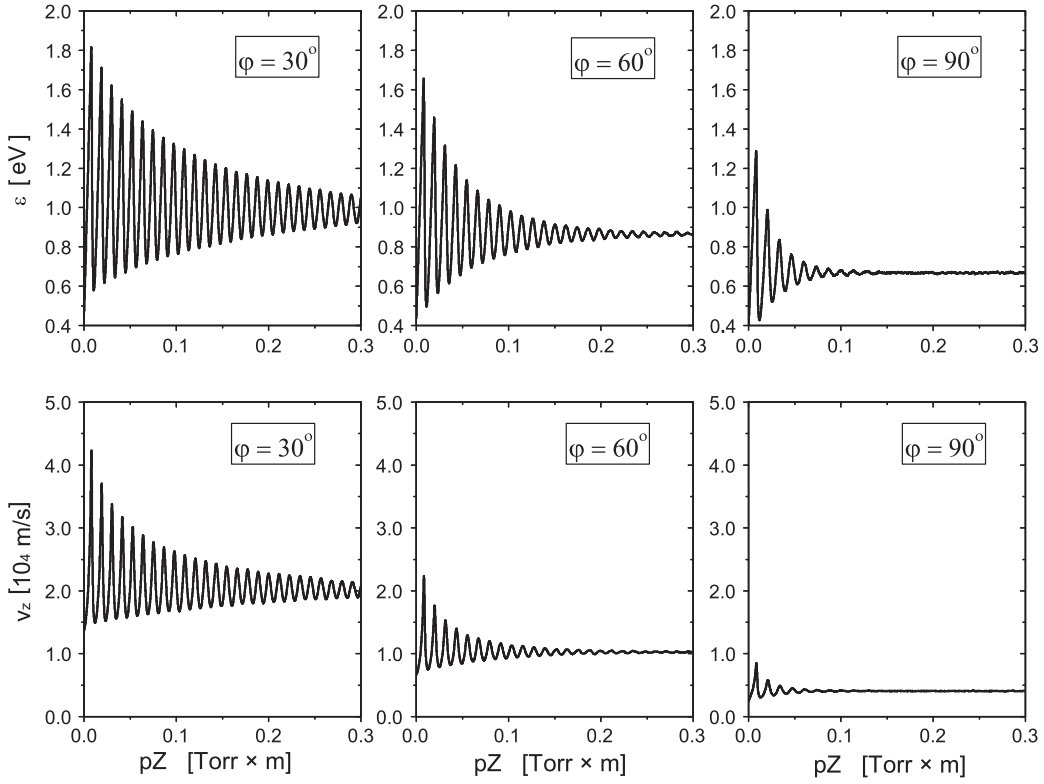

Fig. 6. Spatial relaxation of the mean energy and longitudinal average velocity component for the step model for various field orientations.

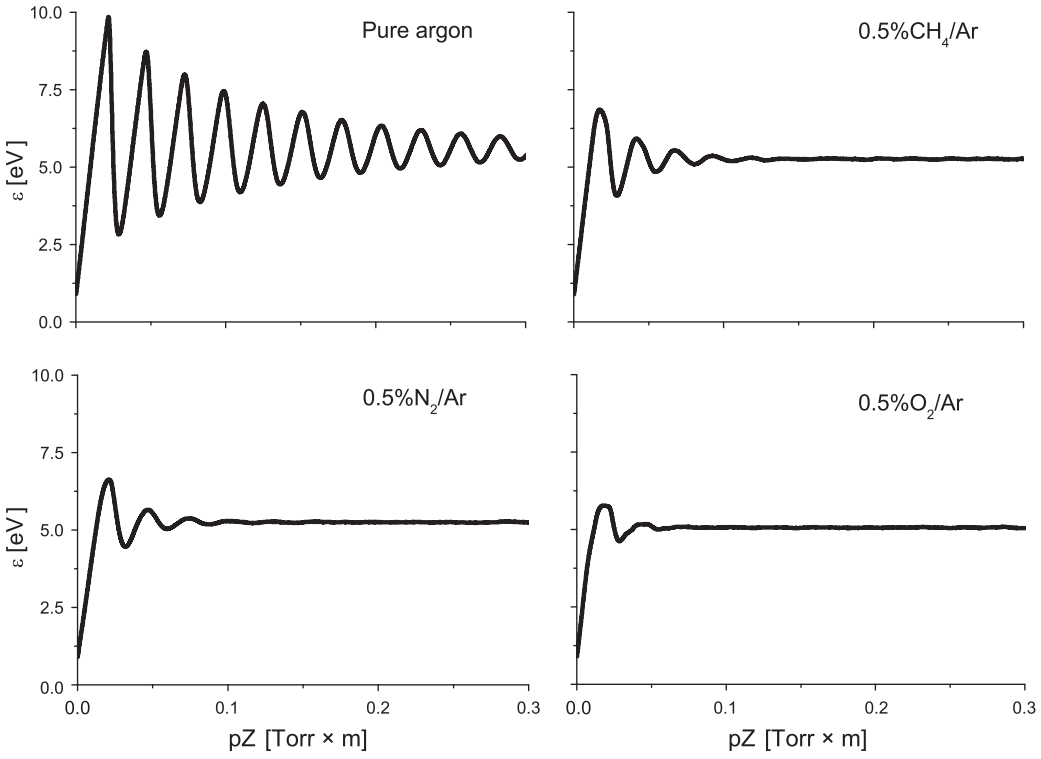

Fig. 7. Spatial relaxation of the mean energy for electrons in argon–CH_4, N_2, and O_2 mixtures for E/n_0 of 15 Td.

m_0 is the mass of the background neutral particles while T_0 is the temperature of the background gas.

Fig. 6 displays the spatial relaxation of the mean energy and longitudinal drift velocity components as a function of the angle between the fields, for B/n_0 of 500 Hx. For parallel fields ($\psi = 0^\circ$), the spatial relaxation profiles of the mean energy and average velocity v_z are in excellent agreement with those associated with a pure electric field. This follows from the symmetry property outlined by White et al. [17]. These general properties were demonstrated under hydrodynamic conditions and as demonstrated here carry over to the case where non-hydrodynamic conditions prevail. The same symmetry properties impose the following: $v_x = v_y$ for $\psi = 0^\circ$ and $v_y = 0$ for $\psi = 90^\circ$. For parallel fields, on average the electrons are traveling in the direction of the electric and magnetic field and hence the magnetic field has no explicit effect. Under the same field orientation, we observe that both ε and v_z exhibit a damped oscillatory relaxation along a decaying profile for a chosen set of conditions. However, as the angle between the fields increases, both the maximal and spatially independent (steady-state) values of ε and v_z are lower than those for parallel fields. The physical mechanism for the cooling action of a magnetic field when electric and magnetic fields are crossed at an arbitrary angle has been detailed in our previous publications [17,18]. In brief, the cooling mechanism is enhanced as the component of the magnetic field perpendicular to the electric field (and hence the angle between the fields) is increased. This means that the cooling mechanism is the strongest in the limit of a crossed field configuration.

In Fig. 7 we show the spatial relaxation of the mean energy in pure argon and mixtures of argon and CH_4, argon and N_2 and argon and O_2. The cross sections for argon are developed by Hayashi [36], the cross sections for CH_4 are displayed and detailed in [37], while the cross sections for N_2 and O_2 are developed by Stojanović and Petrović [32] and Itikawa [38], respectively. We observe that the mean energy in pure argon exhibits a damped oscillatory relaxation along a decaying profile. However, by introducing a small amount of molecular admixture, the oscillations are in the first stage suppressed and then entirely quenched. We see that the most efficient quencher is O_2. This suggest that presence of low threshold rotational and vibrational molecular excitation processes are very efficient in damping by virtue of larger and different energy loss mechanism comparing to elastic collisions. Similar effects have been observed experimentally. Fletcher showed that by introducing a small amount of N_2 in low current, low pressure and steady-state discharges in helium, neon and argon, the existing luminous layers throughout the inter-electrode space can be quenched [39].

4. Conclusion

In this work we have briefly presented a systematic multi-term solution of the non-conservative Boltzmann equation in the time-dependent hydrodynamic and steady-state non-hydrodynamic regimes when both the electric and magnetic fields are present and crossed at arbitrary angles. Our Monte Carlo simulation technique is also presented under the same conditions and applied in parallel with the Boltzmann equation analysis to a series of model and real gases to identify the key issues associated with the correct treatment of temporal and spatial non-locality of electron swarms in varying configurations of electric and magnetic fields in the presence of non-conservative collisions. The importance of treating ionization as a true non-conservative and particle producing process has been demonstrated through the studies of spatiotemporal evolution of the density profile and average energy along the swarm for the ionization model of Lucas and Saelee. The transient spatial structures in the energy distribution functions are reflected in the transient spatial structures in the density profiles – the nature of which is similar to those observed in the steady-state Townsend and Franck–Hertz experiments. Our results indicate that care must be taken to interpret phenomena in transport properties measured under different experimental arrangements, particularly

when electron transport is greatly affected by non-conservative collisions.

Acknowledgements

S.D., Z.M.R. and Z.Lj.P. are supported by the Ministry of Education and Science of Republic of Serbia through the project OI171037 and III41011. S.D. and R.D.W. acknowledge support from the Australian Research Council and the Center for Antimatter-Matter studies, Australia. S.D. also acknowledges support from STW-Project 10118, part of the Netherlands' Organization for Scientific Research (NWO).

References

[1] R.D. White, R.E. Robson, S. Dujko, P. Nicoletopoulos, B. Li, J. Phys. D: Appl. Phys. 42 (2009) 194001.
[2] Z.Lj. Petrović, S. Dujko, D. Marić, G. Malović, Ž. Nikitović, O. Šašić, J. Jovanović, V. Stojanović, M. Radmilović-Radjenović, J. Phys. D: Appl. Phys. 42 (2009) 194002.
[3] T. Makabe, Z.Lj. Petrović, Plasma Electronics: Applications in Microelectronic Device Fabrication, Taylor & Francis Group, New York, 2006.
[4] M.A. Liebermann, A.J. Lichtenberg, Principles of Plasma Discharges and Materials Processing, Wiley, New York, 1994.
[5] R. Winkler, D. Loffhagen, F. Sigeneger, Appl. Surf. Sci. 192 (2002) 50.
[6] R. Winkler, S. Arndt, D. Loffhagen, F. Sigeneger, D. Uhrlandt, Contrib. Plasma Phys. 44 (2004) 437.
[7] W. Blum, L. Rolandi, Particle Detection with Drift Chambers, Springer, Berlin, 1993.
[8] Z.Lj. Petrović, Z.M. Raspopović, S. Dujko, T. Makabe, Appl. Surf. Sci. 192 (2002) 1.
[9] S. Dujko, Z.M. Raspopović, Z.Lj. Petrović, T. Makabe, IEEE Trans. Plasma Sci. 31 (2003) 711.
[10] R.D. White, S. Dujko, K.F. Ness, R.E. Robson, Z.M. Raspopović, Z.Lj. Petrović, J. Phys. D: Appl. Phys. 41 (2008) 025206.
[11] R.D. White, S. Dujko, R.E. Robson, Z.Lj. Petrović, R.P. McEachran, Plasma Sources Sci. Technol. 19 (2010) 034001.
[12] S. Dujko, R.D. White, Z.Lj. Petrović, R.E. Robson, Plasma Sources Sci. Technol. 20 (2011) 024013.
[13] J. Li, Q.M. Chen, J. Phys. D: Appl. Phys. 26 (1993) 1541.
[14] S. Dujko, Ph.D. Thesis, James Cook University, Australia
[15] M. Ould Mohamed Mahmoud, M. Yousfi, J. Appl. Phys. 81 (1997) 5935.
[16] K.F. Ness, Phys. Rev. E 47 (1993) 327.
[17] R.D. White, K.F. Ness, R.E. Robson, B. Li, Phys. Rev. E 60 (1999) 2231.
[18] S. Dujko, R.D. White, Z.Lj. Petrović, R.E. Robson, Phys. Rev. E 81 (2010) 046403.
[19] B. Li, R.E. Robson, R.D. White, Phys. Rev. E 74 (2006) 026405.
[20] B. Li, R.D. White, R.E. Robson, J. Phys. D: Appl. Phys. 35 (2002) 2914.
[21] S. Dujko, R.D. White, Z.Lj. Petrović, J. Phys. D: Appl. Phys. 41 (2008) 245205.
[22] A. Takeda, N. Ikuta, Electr. Eng. Jpn. 164 (2008) 8.
[23] J. Lucas, H Saelee, J. Phys. D: Appl. Phys. 8 (1975) 640.
[24] H. Date, P.L.G. Ventzek, K. Kondo, H. Hasegawa, M. Shimozuma, H. Tagashira, J. Appl. Phys. 83 (1998) 4024.
[25] L. Boltzmann, Wein. Ber. 66 (1872) 275.
[26] C.S. Wang-Chang, G.E. Uhlenbeck, J. DeBoer, in: J. DeBoer, G.E. Uhlenbeck (Eds.), Studies in Statistical Mechanics, vol. 2, Wiley, New York, 1964, p. 241.
[27] K.F. Ness, R.E. Robson, Phys. Rev. A 34 (1986) 2185.
[28] R.E. Robson, K.F. Ness, Phys. Rev. A 33 (1986) 2086.
[29] K. Kumar, H.R. Skullerud, R.E. Robson, Aust. J. Phys. 33 (1980) 343.
[30] R.E. Robson, Aust. J. Phys. 44 (1991) 685.
[31] R.D. White, K.F. Ness, R.E. Robson, Appl. Surf. Sci. 192 (2002) 26.
[32] V.D. Stojanović, Z.Lj. Petrović, J. Phys. D: Appl. Phys. 31 (1998) 834.
[33] Y. Sakai Y, H. Tagashira, S. Sakamoto, J. Phys. B Atom. Mol. Phys. 5 (1972) 1010.
[34] R.E. Robson, B. Li, R.D. White, J. Phys. B: At. Mol. Opt. Phys. 33 (2000) 507.
[35] R.E. Robson, K.F. Ness, J. Chem. Phys. 89 (1988) 4815.
[36] M. Hayashi, personal communication.
[37] O. Šašić, G. Malović, A. Strinić, Ž. Nikitović, Z.Lj. Petrović, New J. Phys. 6 (2004) 74.
[38] Y. Itikawa, J. Phys. Chem. Ref. Data 38 (2009) 1.
[39] J. Fletcher, J. Phys. D: Appl. Phys. 18 (1985) 221.